INTERNATIONAL
Agrophysics
www.international-agrophysics.org

Int. Agrophys., 2026, 40, 423-435
doi: 10.31545/intagr/224655

Net radiation estimation using the Brunt equation for clear sky emissivity and air and canopy temperatures for longwave radiation in well watered crops**

Thiago F. Duarte[1], Xuejun Dong[2], Daniel Leskovar[2], Uzair Ahmad[2], Tonny Jose A.D. Silva[1], Edna Maria B. Silva[1], Noemi Tortorici[3]*

[1]Institute of Agricultural and Technological Sciences, Federal University of Rondonópolis, Avenida dos Estudantes, 5055, Cidade Universitária, Rondonópolis, MT, Brazil
[2]Texas A&M AgriLife Research and Extension Center at Uvalde, 1619 Garner Field Road, Uvalde, Texas 78801, United States
[3]Dipartimento di Scienze Agrarie, Alimentati e Forestali, Università degli Studi di Palermo, Italy

Received April 2, 2026; accepted June 16, 2026

Abstract. Net radiation (R_n) is commonly estimated using models that apply the Brunt equation to calculate incoming longwave radiation and use air temperature (T_{air}) to estimate outgoing longwave radiation under reference conditions. This study evaluated two previously calibrated Brunt models to estimate R_n without site-specific calibration and assessed whether T_{air} can substitute for canopy temperature (T_c) under well-watered crop conditions. Measurements were collected in sesame and cotton fields during the first year and in a cotton field during the second year, when T_c was also measured. Net radiation was estimated at hourly and daily time scales. Across all methods, errors were higher at the hourly scale than at the daily scale. Daily-scale performance metrics showed *RMSE* values of 11.88 and 13.45 W m^{-2} and *KGE* values of 0.91 and 0.74 for the first and second years, respectively. Both regionally calibrated Brunt models outperformed the Allen/FAO method. Although statistical differences were detected between R_n estimates derived from T_{air} and T_c, regression analyses and error metrics indicated that these differences were small, particularly at the daily scale. Therefore, the calibrated Brunt equations effectively improve R_n estimation, and T_{air} can reliably replace T_c for daily R_n calculations under well-watered conditions.

Keywords: energy balance, radiation balance, biophysical models, Penman-Monteith

1. INTRODUCTION

Net radiation (R_n) results from the radiation balance at a specific site, where the downward radiation fluxes reaching the ground surface are balanced by the upward reflected shortwave radiation and emitted longwave radiation from the surface. It represents the amount of energy available to drive biophysical processes such as latent heat flux, sensible heat flux, and soil heat flux. Consequently, R_n is generally required as an input variable for biophysical models based on the energy balance concept. For example, R_n is a required input variable for all the following models: the canopy stomatal conductance model proposed by Blonquist Jr. *et al.* (2009), the original crop water stress index (CWSI) model derived by Jackson *et al.* (1981), the Penman-Monteith equation (Allen *et al.,* 1998), and the approach for modeling the soil temperature developed by Holmes *et al.* (2008).

*Corresponding author e-mail: thiago.duarte@ufr.edu.br
**This work was supported by Texas A&M AgriLife Research Cropping System Program (Leskovar), Sesaco Co. Uvalde Field Trial project (Dong and Leskovar), Cotton Incorporated/Texas State Support Committee project 20-557TX (Dong), USDA-NIFA Hatch project 9574-2 (Dong), USDA Multi-State Specialty Crop Project TX-SCMP-19-01 (Leskovar), and Brazilian Federal Agency for Support and Evaluation of Graduate Education (CAPES/ PRAPG) Notice 14/2023 (Duarte). The work also received support from University of Palermo, Italy for Tortorici to visit Uvalde Research Center.

Despite its importance, R_n is not always measured directly, mainly because it is expensive and difficult to measure accurately (Blonquist Jr. *et al.,* 2010). One primary challenge is the measurement footprint, as net radiometers must be positioned to capture the heterogeneity of canopy cover representatively, which can vary significantly in row crops. Furthermore, these sensors are highly sensitive to leveling errors, require frequent dome maintenance to prevent dust interference, and are prone to substantial long-term calibration drift. In such cases, R_n must be estimated using theoretical or empirical models. The basic theoretical equation for estimating R_n consists of two components: net shortwave radiation (S_n) and net longwave radiation (L_n). The calculation of S_n is usually straightforward, as it depends on the incoming shortwave radiation and surface albedo – data that are commonly available. However, calculating the L_n component is more challenging because it depends on the atmospheric composition and temperature, which are needed to estimate the incoming longwave radiation, as well as on surface temperature, which is required to estimate the emitted longwave radiation – variables that are not routinely available.

When modeling the incoming longwave radiation, sky emissivity (ε_{sky}) is typically estimated based on near-surface air temperature and vapor pressure, and sky temperature is replaced by the air temperature at the same reference height (Jensen and Allen, 2016). Sky emissivity is calculated using clear-sky emissivity models (ε_c) adjusted by cloud fraction, since the presence of clouds significantly increases sky emissivity. Several models have been developed to calculate ε_c, as reviewed by Flerchinger *et al.* (2009), Formetta *et al.* (2016), and Li *et al.* (2017), and models' performance is generally improved after proper calibration. However, after working with fifteen models to estimate ε_c in the United States, Li *et al.* (2017) concluded that although these models have different functional forms and coefficients, most of them exhibit similar accuracies after calibration and can be grouped into only two families of models, the Brunt type (Brunt, 1932) and the Carmona type (Carmona *et al.,* 2014). Moreover, because the calibrated Brunt model has the simplest functional form and is among the most accurate, it can be recommended as a reference for calculating ε_c.

Similarly to sky temperature, surface temperature is not routinely measured, and its substitution is complex and should be applied with caution, as it depends on several factors such as ground cover type, soil type, soil water content, and others. Under reference conditions, as described by Jensen and Allen (2016), where the surface evaporates and transpires at rates corresponding to reference evapotranspiration, surface temperature (T_s) is sufficiently close to air temperature (T_{air}); therefore, T_s can be approximated by T_{air}. For non-reference conditions, however, this approach is generally not recommended, particularly when the surface is dry and hot. Alternatively, surface temperature can be simulated using numeric methods, such as Newton's iterative method (Bristow, 1987) or the iterative solution of aerodynamic fluxes (Jensen and Allen 2016). Nevertheless, these approaches significantly increase the complexity of R_n estimation, especially at shorter time-scales, as they require air-stability correction for calculating aerodynamic resistance as well as proper estimation of bulk surface resistance. In addition, using simulated T_s may introduce errors that could propagate uncertainty in the R_n estimation. Thus, in cases where a simple approach of approximating T_s by T_{air} is suitable, it should be preferred for R_n estimation.

In this sense, for example, An *et al.* (2017) reported that substituting soil temperature for air temperature in net radiation estimates over an experimental embankment did not significantly affect the results at half-hourly and hourly scales. Conversely, in his classical work, Linacre (1969) found that for monthly estimates of net radiation, approximating T_s by T_{air} led to significant errors across different soil types. More recently, Pieri (2010) developed a net radiation partition model applied to grapevines and reported that substituting leaf temperatures with air temperature measured near the canopy had only a minor impact on model performance.

In this study, net radiation was measured in irrigated cotton and sesame fields over two years: 2015 (sesame and cotton) and 2025 (cotton). In the second year, canopy temperature was also measured, beginning at the nearly full canopy stage. Under this condition, we assumed that the surface temperature could be represented by the canopy temperature (T_c). The primary objective of this research was to evaluate the accuracy of net radiation (R_n) estimation models that utilize air temperature (T_{air}) as a surrogate for canopy temperature (T_c) under well-watered conditions. To achieve this, we first assessed whether surface temperature could be replaced by air temperature without a significant loss of accuracy, as is commonly assumed in net radiation studies involving reference crops. Additionally, we aimed to determine if R_n estimation could be improved by utilizing broadly calibrated clear-sky emissivity (ε_c) equations, specifically the Brunt-type models from Formetta *et al.* (2016) and Li *et al.* (2017), to eliminate the requirement for site-specific calibration. These studies were selected for two reasons. First, Formetta *et al.* (2016) performed calibrations for several U.S. states, including Texas – where this study was conducted – and generated regionally specific calibrated parameters. Second, to test whether a more general or universal calibration equation would result in accurate longwave radiation estimation, the model of Li *et al.* (2017) was selected, as their equation was derived from grouped data from a large dataset collected across the United States. By validating these pre-calibrated equations and examining the temperature substitution limits, this study contributes to simplifying the data requirements of biophysical and energy balance models. It demonstrates that highly accessible meteorological data can substitute for specialized canopy-level measurements without a significant loss of accuracy, thereby reducing the barriers to implementing evapotranspiration and crop water stress models.

2. MATERIALS AND METHODS

2.1. Locality and measurements

The study was carried out in a farm field at the Texas A&M AgriLife Research and Extension Center at Uvalde. The local soil is Fine-silty, mixed, active, hyperthermic Aridic Calciustoll (https://soilseries.sc.egov.usda.gov/OSD_Docs/U/UVALDE.html), and the climate is classified as Humid Subtropical climate (Cfa) according to the Köppen climate classification system.

The net radiation measurements were performed in 2015 and 2025. In 2015, the measurements were taken in a 4.9 ha cotton crop field from 7/15/2015 to 9/4/2015 and in a 4.9 ha sesame crop field from 9/4/2015 to 10/29/2015. The two crop fields were located about 80 m from each other within a 20 ha field irrigated using a center pivot system. Cotton (variety PHY 499 WRF) was cultivated from 04/02/2015 to 09/23/2015, with 1.02 m row spacing and a stand of 100 000 pl ha^{-1}, and during the net radiation measurements the leaf area index changed from 4.85 to 3.49 m^2 m^{-2}. Sesame (variety S36 from Sesaco Co. San Antonio, TX, USA) was cultivated from 7/16/2015 to 11/23/2015, with 1.02 m row spacing and a stand of 450,000 pl ha^{-1} with the leaf area index changing from 4.86 to 1.49 m^2 m^{-2} during the measurements (Fig. 1). In 2025, the net radiation measurements were taken only in a cotton field, from the period of 6/19/2025 to 9/02/2025, with the leaf area varying from 1.5 to 3.8 m^2 m^{-2} (Fig. 1). Similarly to 2015, the cotton (varieties NG 4190 and ST 4990) was planted with 0.76 m row spacing and a stand of 129 000 pl ha^{-1}. Leaf area index for the cotton crop in both years was measured using a LI-2200C Plant Canopy Analyzer (LI-COR, Inc. Lincoln, NE, USA) on relatively calm days without significant amounts of broken clouds in the sky. The LAI for the sesame crop was estimated using the field-measured data of oven-dried green leaf mass per unit land area multiplied by the specific leaf area.

In both years, the crops were irrigated to meet crop water demand, calculated based on maximum evapotranspiration. In 2015, a center-pivot irrigation system was used, while a dripline system was used in 2025.

In both 2015 and 2025, the net radiation measurements were performed using an NR-Lite2 Net Radiometer sensor (Kipp and Zonen, Delft, The Netherlands) installed at a height of 3.0 m above the ground surface, with data collected at 1 min intervals. In 2015, the data was recorded using a LOGBOX SD datalogger (Kipp and Zonen, Delft, The Netherlands), while in 2025 the measurement was made using a CR1000 datalogger (Campbell Scientific, Logan, Utah, USA). Additionally, solar radiation (W m^{-2}), air temperature (°C), and relative humidity (%), were measured at 5 min intervals at an automatic weather station located within 500 m from the experimental site. Net radiation data collected at 1 mine intervals and weather station data collected at 5 min intervals were averaged to create hourly values for use in the shorter time scale model evaluations. In 2025, canopy temperature was also measured using a set of infrared radiometers (SI-111-SS and SI-131-SS; Apogee Instruments, Inc., Logan, Utah, USA) at 15-minute intervals via a CR1000 datalogger. Measurements were obtained using two sensors installed approximately 50 cm apart and 15 cm above the top of the canopy. The sensors were tilted at approximately a 35° angle relative to the vertical axis, with one sensor directed toward the west side, and the other toward the east side on one representative cotton row (Fig. 2). One advantage of tilting the sensors was to avoid soil surface exposure to the sensors' field of view. The average of the two measurements was then calculated and used to estimate the longwave radiation emitted by the cotton canopy, as described in the next section.

2.2. Net radiation models

The basic equation to estimate R_n can be described as below (Monson and Baldocchi, 2014):

$$R_n = (1 - \alpha)R_s - \varepsilon_s \sigma (T_s)^4 + \varepsilon_{sky} \sigma (T_{air})^4, \quad (1)$$

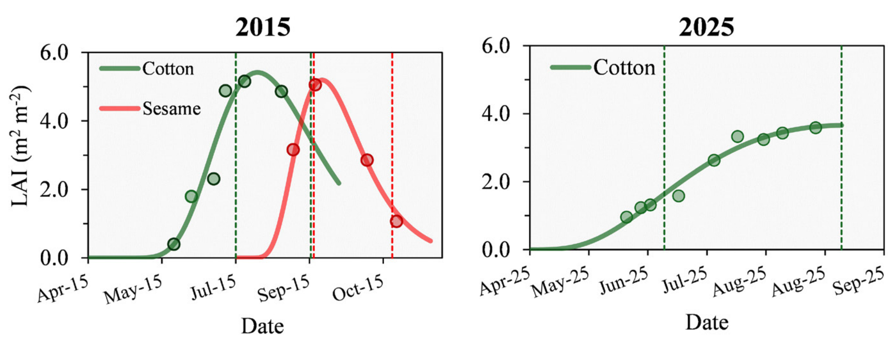

Fig. 1. Leaf area index variations in cotton and sesame plots during the crop cycle in which the net radiation was measured in 2015 and 2025 at the Uvalde Research Center. The vertical dashed lines represent the period of net radiation measurement.

Fig. 2. Details of the installation of the infrared radiometer sensors in the cotton field at the Uvalde Research Center in 2025. Shown in the background is the NR-Lite2 net radiometer mounted on a metal pole.

where: R_n – net radiation (W m^{-2}), α – surface albedo, defined as 0.21, R_s – solar radiation (W m^{-2}), ε_s – surface emissivity, ε_{sky} – sky emissivity, σ – Stefan-Boltzmann constant (5.670 × 10^{-8} W m^{-2} K^{-4}), T_s – surface temperature (K), T_{air} – air temperature (K).

Eq. (1) can be simplified to the following equations:

$$R_n = S_n - L\uparrow + L\downarrow, \tag{2}$$

$$R_n = S_n + L_n, \tag{3}$$

where: S_n – net shortwave radiation (W m^{-2}), $L\uparrow$ – upward longwave radiation (W m^{-2}), $L\downarrow$ – downward longwave radiation (W m^{-2}), L_n – net longwave radiation (W m^{-2}).

In this work, net radiation was calculated in hourly and daily time scales using different approaches described in detail in the following sections. The difference between the methods lies in how L_n was calculated, either by altering $L\downarrow$ or by altering $L\uparrow$. The method proposed and described by Allen *et al.* (1994) was considered the standard method. In 2015, as canopy temperature measurements were not available, only different $L\downarrow$ models were tested. In 2025, the $L\uparrow$ component was estimated based on measured canopy temperatures, and $L\downarrow$ was also tested using different models.

2.2.1. FAO-Allen *et al.* (1994) model

In the Allen *et al.* (1994) model, net radiation is estimated on a daily time scale using Eq. (4), with its supporting components (e_d, R_{so}, and R_a) calculated through Eqs (5) to (9):

$$R_n = (1-\alpha)R_s - \left[a_c\left(\frac{R_s}{R_{so}}\right) + b_c\right] \times \left(a_1 + b_1 e_d^{0.5}\right)\sigma\left(\frac{T_m^4 + T_n^4}{2}\right), \tag{4}$$

where: R_n – net radiation (W m^{-2}); α – surface albedo, defined as 0.21; R_s – solar radiation (W m^{-2}); R_{so} – clear-sky solar radiation (W m^{-2}); e_d – vapor pressure at the dew point (kPa); T_m – maximum air temperature (K); T_n – minimum air temperature (K); a_c and b_c are the cloud factors, 1.35 and -0.35, respectively (-); a_1 and b_1 – area emissivity factors, defined as 0.35 and – 0.14; σ – Stefan-Boltzmann constant (5.670 × 10^{-8} W m^{-2} K^{-4}).

The variables e_d and R_{so} can be calculated using Eqs (5) and (6) as follows:

$$e_d = 0.611\exp\left(\frac{17.27T_d}{T_d + 237.3}\right), \tag{5}$$

$$R_{so} = (0.75 + 2 \times 10^{-5}z)R_a, \tag{6}$$

where: T_d – dew point temperature (°C), z – is the elevation above the sea level (m), R_a – extraterrestrial solar radiation (W m^{-2}). The R_a in turn is calculated using Eqs (7)-(9):

$$R_a = \left[\frac{24 \times 60}{\pi}\right] \times G_{sc} d_r (cos\emptyset cos\delta sin\omega_s + \omega_s sin\emptyset sin\delta), \tag{7}$$

$$d_r = 1 + 0.033cos\left(\frac{2\pi J}{365}\right), \tag{8}$$

$$\omega_s = cos^{-1}(-tan\emptyset tan\delta), \tag{9}$$

in which G_{sc} is the solar constant (1 367 W m^{-2}), d_r is the relative distance between the Earth and the sun (1.496 × 10^{11} m), J is the Julian day of year, ω_s is the sunset time angle (rad), ϕ and δ are the latitude (rad) and solar declination (rad).

The previous equations are adjusted for shorter timescales (hourly or sub-hourly) to calculate solar radiation on a horizontal surface as follows (Allen *et al.*, 1994; An *et al.*, 2017):

$$R_n = (1-\alpha)R_s - \left[a_c\left(\frac{R_s}{R_{so}}\right) + b_c\right] \times \left(a_1 + b_1 e_d^{0.5}\right)\sigma\left(T_a^4\right), \tag{10}$$

$$R_{sa} = \left[\frac{24 \times 60}{\pi}\right] G_{sc} d_r \times [cos\emptyset cos\delta(sin\omega_2 - sin\omega_1) + (\omega_2 - \omega_1)sin\emptyset sin\delta], \tag{11}$$

$$\omega_1 = \omega - \frac{\pi}{\frac{24}{\tau}}, \tag{12}$$

$$\omega_2 = \omega + \frac{\pi}{24/\tau}, \tag{13}$$

where: T_a – mean air temperature (K), ω_1 and ω_2 are the solar time angles (rad) at the beginning and end of the considered period, ω is the solar time angle (rad) at the center of the period, and τ is the length of the period (h).

In Eqs (5) and (11), the term $f = a_c\left(\frac{R_s}{R_{so}}\right) + b_c$ represents the cloudiness function. The approach of Snyder and Eching (2002) was applied in this study with the restriction of $0.3 < R_s/R_{so} \leq 1.0$ and $R_s/R_{so} = 0$ whenever $\beta < 17.5°$. Furthermore, an initial f value of 0.6 was used, and for each sequential data, whenever $\beta < 17.5°$, the f value was set equal to the previous f value, and β represents the solar altitude:

$$\beta = \frac{180}{\pi} sin^{-1}[sin\emptyset sin\delta + cos\emptyset cos\delta cos\omega]. \tag{14}$$

2.2.2. Testing different sky emissivity models

The main challenge for the calculation of downward longwave radiation is the determination of sky emissivity. In this work, we tested the Brunt model for calculating clear-sky emissivity as calibrated by Formetta *et al.* (2016) and Li *et al.* (2017), as presented in Table 1. Although both models share a similar linear functional form based on the square root of vapor pressure, as pointed out before, these references were selected because they provide two options for ε_{sky} calculation: one that is more regionally specific and another that is more universal, respectively.

Since the Brunt model is only valid for clear sky conditions, the correct estimation of downward longwave radiation for all-sky conditions requires considering the contribution of clouds. For this purpose, the Crawford and Duchon (1999) model was tested in this work:

$$L\downarrow = [clf + (1 - clf)\varepsilon_c]\sigma T_{air}^4, \tag{15}$$

$$L\downarrow = \varepsilon_{sky}\sigma T_{air}^4, \tag{16}$$

where: clf is the cloud fraction term, ε_{sky}=[clf+(1-clf) ε_c], and ε_c is the clear-sky emissivity.

The clf was calculated as $clf = 1 - s$, where s represents the ratio between solar radiation measured at the weather station (W m^{-2}) to the clear-sky radiation. The clear-sky radiation component can be calculated by several models, such as Jensen *et al.* (1990), Crawford and Duchon (1999), and Li *et al.* (2017). In this work, the same approach as that used in Eqs (5) and (11), that is, $s = R_s/R_{so}$, was employed.

2.2.3. Estimating the upward longwave radiation

This approach differs from the previous two in that it uses the canopy temperature measurements to calculate upward longwave radiation, and it was tested only with the 2025 data. Thus, the downward longwave radiation was calculated using the same equations described in the previous section, and the $L\uparrow$ component was calculated as presented in Eqs (1) and (2). The parameter ε_s was set to 0.96, a representative value for the cotton crop (Campbell and Norman, 1998).

2.3. Statistical analysis

The net radiation methods described in the previous section were evaluated in two steps: hourly and daily timescales. The measured and simulated data were compared using the root mean square error (*RMSE*), mean absolute error (*MAE*) Bias, and the Kling-Gupta efficiency (*KGE*), as described below (Gupta *et al.,* 2009; Moriasi *et al.,* 2007):

$$RMSE = \sqrt{\frac{1}{n}\sum_{i=1}^{n}(P_i - O_i)^2}, \tag{17}$$

$$MAE = \frac{1}{n}\sum_{i=1}^{n}|P_i - O_i|, \tag{18}$$

$$Bias = \frac{1}{n}\sum_{i=1}^{n}(P_i - O_i), \tag{19}$$

$$KGE = 1 - \sqrt{(r-1)^2 + (\alpha - 1)^2 + (\zeta - 1)^2}, \tag{20}$$

$$r = \frac{\sum(O_i - \bar{O})(P_i - \bar{P})}{\sqrt{\sum(O_i - \bar{O})^2 \sum(P_i - \bar{P})^2}}, \tag{21}$$

Table 1. Brunt equation with different parameters calibrated by Formetta *et al.* (2016) and Li *et al.* (2017)

Equation	Period	Reference	Local of calibration	Variable
$\varepsilon_c = 0.62 + 0.16\sqrt{e_a}$	All day	Formetta *et al.* (2016)	Texas, U.S.	e_a (kPa)
$\varepsilon_c = 0.598 + 0.057\sqrt{e_a}$	Daytime	Li *et al.* (2017)	Seven stations Across U.S.	e_a (hPa)
$\varepsilon_c = 0.633 + 0.057\sqrt{e_a}$	Nighttime	Li *et al.* (2017)		e_a (hPa)

ε_c – clear-sky emissivity; e_a – water vapor pressure.

$$\alpha = \frac{\sigma_P}{\sigma_O}, \quad (22)$$

$$\zeta = \frac{\bar{P}}{\bar{O}}, \quad (23)$$

where: O_i is the observed value for the i-th data point, P_i is the predicted value for the i-th data point; $\bar{O}$ is the mean of the observed values; is the mean of predicted values; n is the total number of observations; σ_o is the standard deviation of observations, and σ_P is standard deviation of predictions.

Additionally, the Wilcoxon signed-rank test and Bland-Altman analysis were used to compare R_n estimates derived from T_{air} and T_c. The Wilcoxon test was applied to assess paired differences between the methods using the Minitab 22, while agreement and systematic bias were evaluated using the Bland-Altman approach, calculated as described by Yellareddygari and Gudmestad (2017). The Bland-Altman analysis is a graphical method in which the differences between the R_n methods (Y-axis) and the averages of the methods (X-axis) are plotted on the same graph. The mean difference between the methods (*i.e.*, Bias), and the limits of agreement, calculated as bias ± 1.96 × standard deviation (SD), are also plotted. This method was first used in medicine (Bland and Altman, 1986), but more recently in crop and soil sciences studies (Yellareddygari and Gudmestad, 2017; Lipiec *et al.,* 2021; Usowicz, *et al.,* 2020).

3. RESULTS AND DISCUSSION

The results of net radiation estimation using different approaches for 2015 are presented in Figs 3 and 4, with the corresponding statistical performance shown in Fig. 5. It can be observed that the performance of the methods depends on the timescale, with more accurate values obtained on a daily scale than on an hourly scale. In general, considering all methods, the *RMSE*, *MAE*, *Bias*, and *KGE* values were 38.95, 28.34, -5.49, and 0.90 for hourly time scales, and 11.88, 9.13, 2.53, and 0.91 for daily time scales, respectively. Despite this, the R_n estimates using the approach of Formetta *et al.* (2016) for ε_c were superior to

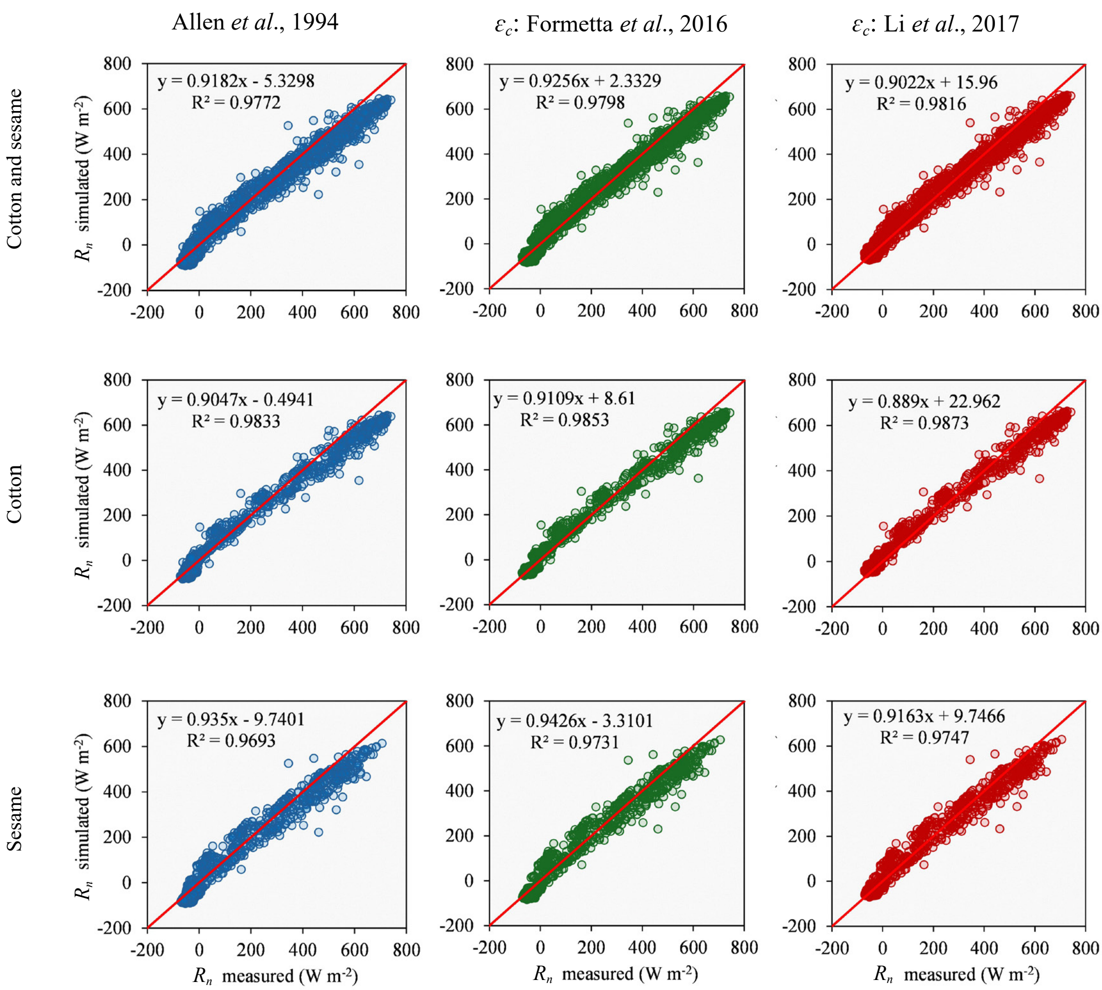

Fig. 3. Relationship between hourly simulated and measured net radiation (W m^{-2}) in cotton and sesame fields at Uvalde in 2015, using different methodologies. ε_c: clear-sky emissivity model.

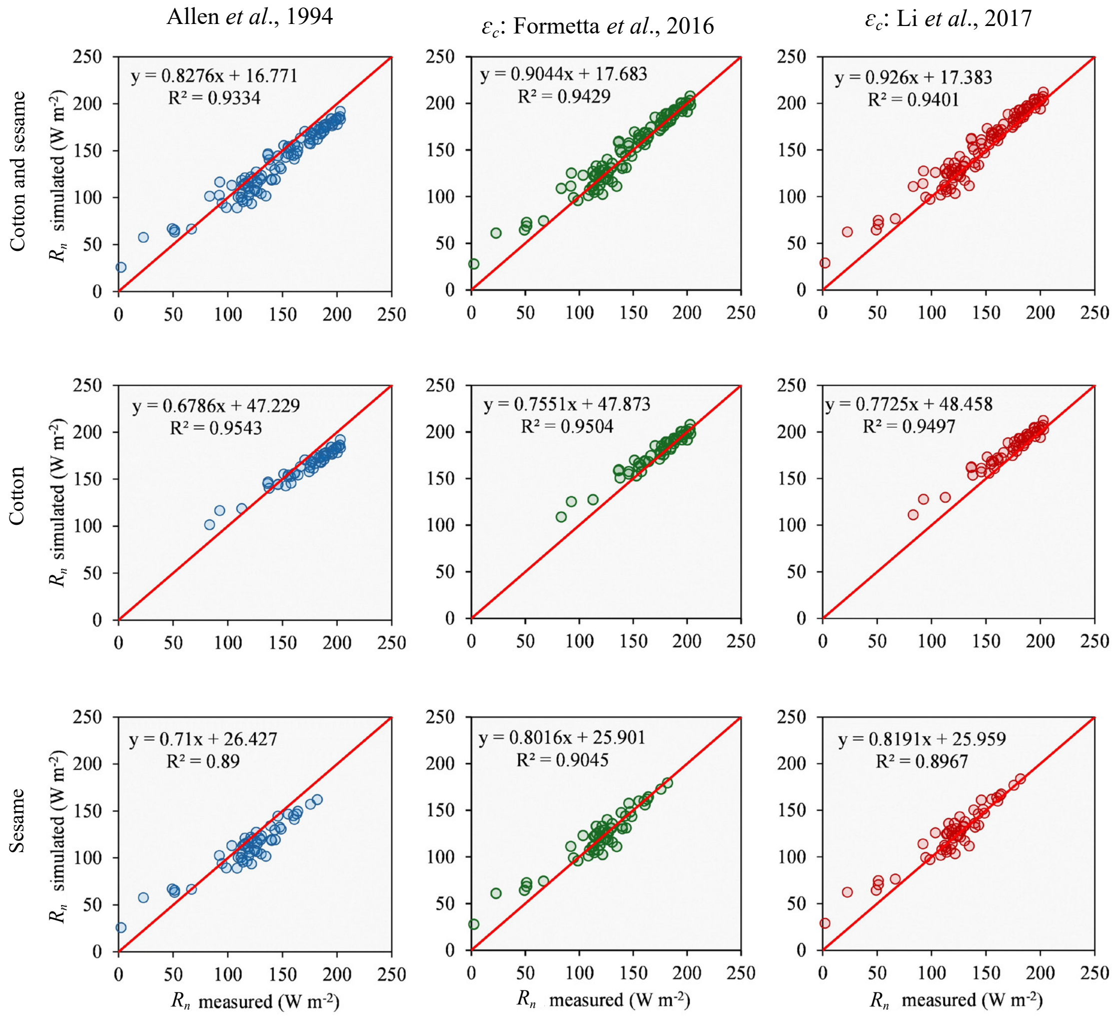

Fig. 4. Relationship between daily simulated and measured net radiation (W m^{-2}) in cotton and sesame fields at Uvalde in 2015, using different methodologies. ε_c: clear-sky emissivity model.

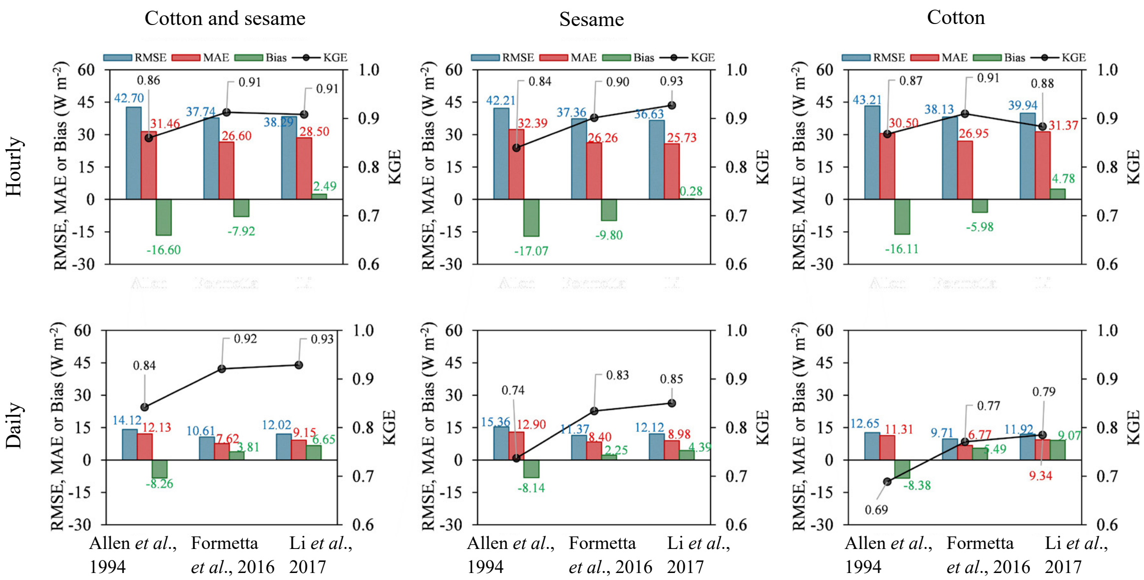

Fig. 5. Statistical performance of net radiation calculation methods at hourly and daily time scales for the year 2015. Coloured values represent the respective statistical metrics.

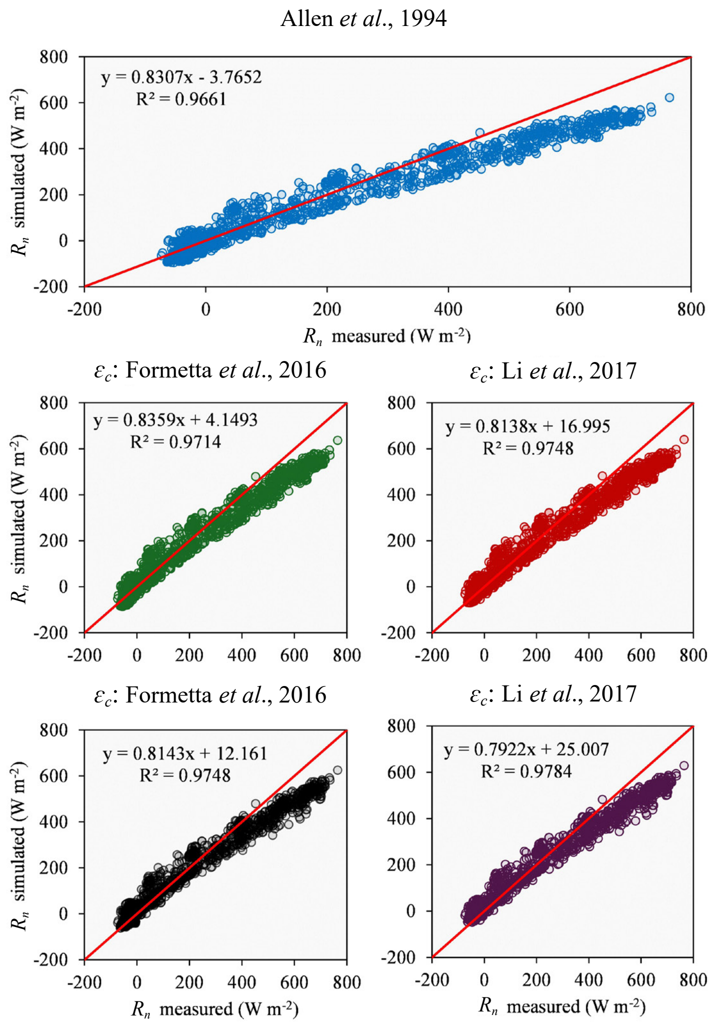

Fig. 6. Relationship between hourly estimated and measured net radiation (W m^{-2}) in cotton field at Uvalde in 2025, using different methodologies. ε_c: clear-sky emissivity model. T_s: surface temperature (°C); Tair: air temperature (°C); T_c: canopy temperature (°C).

those obtained with the other methods, with overall error across both crops of 37.74 (*RMS*E), 26.60 (*MAE*), -7.92 (*Bias*), and 0.94 (*KGE*).

For the year 2025, the errors were slightly higher than those observed in 2015, particularly at the hourly time scale, as shown in Figs 6 to 8. The general errors were 55.94 (*RMSE*), 40.10 (*MAE*), -14 (*Bias*), and 0.81 (*KGE*) for hourly time scales, and 13.45, 10.46, 0.10, and 0.74 for daily time scales, respectively. Nevertheless, both methods used to estimate ε_c outperformed the Allen method with its original calibrated parameters. The differences between the Formetta and Li methods were not very pronounced when using either T_{air} or T_c. However, the Li equation consistently produced lower bias, regardless of the type of temperature that was used (Fig. 8).

The higher errors in simulated R_n at shorter time scales (Figs 5 and 8) can be partially attributed to the assumption of constant albedo throughout the day. In turfgrass, for example, Blonquist Jr *et al.* (2010) found that albedo can vary from 0.21 to 0.30, while in cotton, data presented by Carvalho *et al.* (2022) showed that it can vary by approximately 0.08 units, changing from 0.22 to 0.30 at the flowering stage. However, Blonquist Jr *et al.* (2010) point out that the most critical errors in estimating R_n at short time scales are related to net longwave radiation. In this context, part of the error source can be attributed to the assumption that the cloudiness function remains constant during the night, which can lead to incorrect estimates for those periods. In addition, estimating atmospheric emissivity based on e_a and assuming that T_{air} is representative of atmospheric temperatures may not be suitable in some situations and, consequently, may not accurately capture longwave radiation dynamics.

The performance of R_n estimation could likely have been improved with local, site-specific calibration, as demonstrated in other studies (Kjaersgaard *et al.,* 2007; Myeni *et al.,* 2020). However, one of the aims of this work was to evaluate whether the previously calibrated coefficient could yield acceptable results, thereby eliminating the need for highly site-specific calibration. A similar attempt

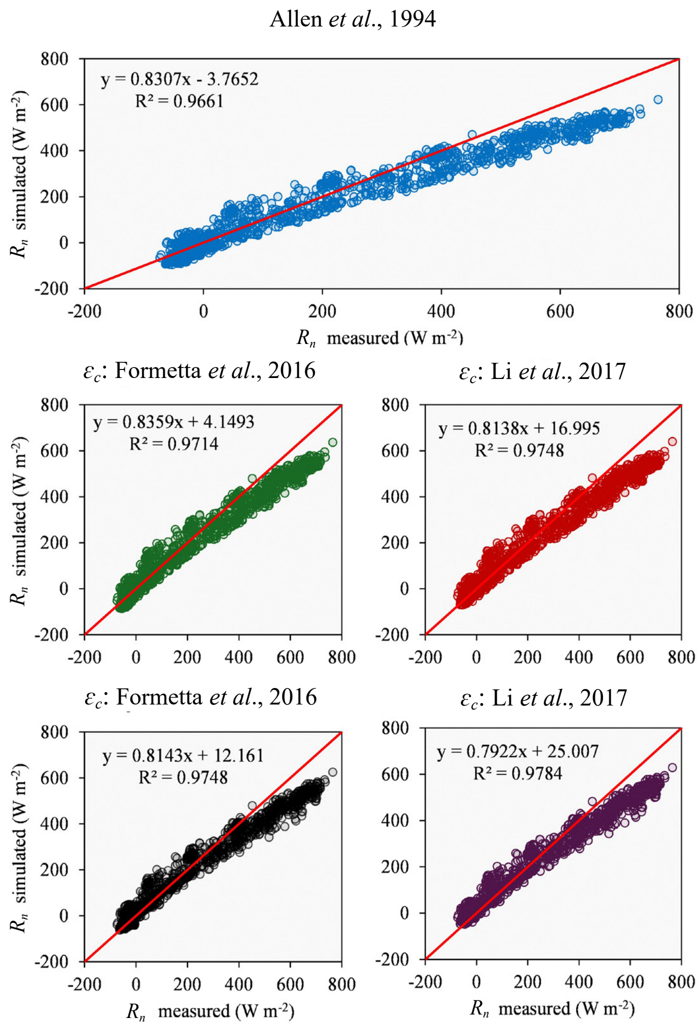

Fig. 7. Relationship between daily estimated and measured net radiation (W m⁻²) in a cotton field during 2025, using different methodologies. ε_c: clear-sky emissivity model; T_s: surface temperature (°C); T_{air}: air temperature (°C); T_c: canopy temperature (°C).

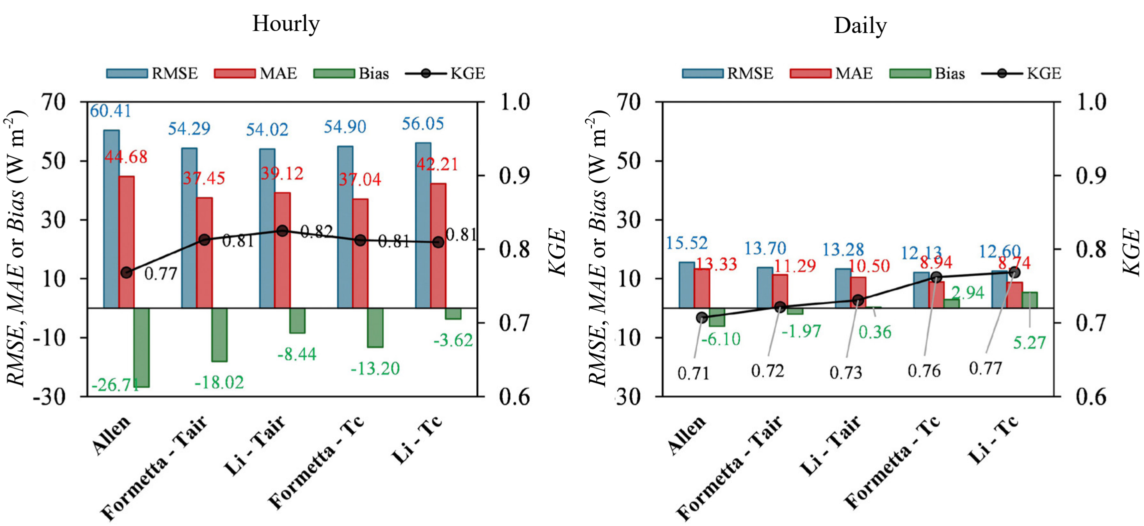

Fig. 8. Performance of net radiation estimation methods across various time scales for the year 2025. Coloured values represent the respective statistical metrics (Allen *et al*., 1994; Formetta *et al*., 2016; Li *et al*., 2017).

Table 2. Results of the Wilcoxon signed-rank test for comparing R_n estimates obtained from T_{air} and T_c

Variable	n	Median	Wilcoxon statistic	p
Hourly (T_{air} *vs* T_c)	1 727	-5.05	343 890	<0.001
Daily (T_{air} *vs* T_c)	72	-4.52	139	<0.001

was made by Myeni *et al.* (2020) for southern African conditions, in which the authors tested whether R_n estimation could be improved using the original equations of Idso and Jackson (1969) or Brutsaert (1975) to estimate clear-sky emissivity in combination with the cloudiness factor model of Crawford and Duchon (1999). Overall, the authors found that the evaluated method outperformed the Allen model in its original form. While other functional forms for emissivity exist, such as the power-law models evaluated by Morales-Salinas *et al.* (2023), the Brunt-type models are frequently recommended as a reference due to their high accuracy and simple functional form after calibration. In this work, we used the Brunt model calibrated by different authors, and although the parameter values differed, their performance was similar and superior to that of the original Allen equation. Thus, both approaches can be used to improve the estimation of clear-sky emissivity and, consequently, net radiation.

The higher errors observed in 2025 may be attributed to the lower LAI compared with 2015 (Fig. 1), which resulted in reduced crop ground cover. Consequently, the fraction of exposed soil may have altered the amount of reflected shortwave radiation, thereby affecting net shortwave and, in turn, R_n. A second source of error may also be attributed to the outward longwave radiation originating from the partially exposed soil surface, which exceeded the contribution accounted for in this study, since soil surface temperature normally differs from canopy temperature and, consequently, alters the emitted longwave radiance.

Bsaibes *et al.* (2009), who analyzed the relationship between LAI and albedo for different crops, observed that, for low to moderate LAI values (LAI < 3), the soil background exerted a stronger influence on albedo values, whereas for larger LAI values, albedo tended toward an asymptotic value that may depend more on canopy characteristics such as architecture, like chlorophyll content, among others. Soil albedo is usually lower than the crop albedo, especially for dark and moist soils (He *et al.,* 2019), with general values ranging from 0.08 (wet, dark soil) to 0.18 (soil, dry light), as pointed out by Campbel and Norman (1998). A higher soil contribution would result in lower shortwave reflectance and, consequently, higher R_n values. In this study, we assumed a fixed albedo value of 0.21 for both years, which may have led to an underestimation of the actual R_n values.

To assess whether canopy temperature (T_c) can be approximated by air temperature (T_{air}) for R_n estimation, the R_n values calculated using both temperatures were compared using the Wilcoxon signed-rank test, as shown in Table 2. The results indicate that, for both time scales, the median difference between R_n estimated using T_{air} and T_c was significantly different from zero. Therefore, strictly speaking, for cotton crops, R_n cannot be estimated by substituting T_c with T_{air}, even under well-watered conditions. However, overall, the error metrics were very similar between the two methods (Fig. 8), with notable differences observed only in the Bias for hourly scale, ranging from -18.02 (T_{air}) to -13.20 (T_c) for Formetta and from -8.44 (T_{air}) to -3.62 (T_c) for Li.

Nevertheless, linear regression analysis between R_n simulated using T_{air} and T_c showed that the regression line was close to the 1:1 line (Fig. 9) for both hourly and daily time scales. For the hourly scale, the slope was close to 1, although the intercept was significantly different from zero, indicating a small systematic bias but an overall good agreement (Table 3). For the daily scale, the intercept did not differ significantly from zero, and the slope was close to 1, demonstrating that the differences between R_n estimated from T_{air} and T_c were negligible.

The Bland-Altman plot (Fig. 10) revealed greater variability at the hourly scale compared to the daily scale. Although most data points were within the limits of agreement (95% of the differences), some estimates fell outside these limits, particularly for extreme R_n values. Conversely, at the daily scale, the errors between the methods appeared to be more uniformly distributed, with noticeable deviations occurring only at higher R_n values. It is interesting to note that the Bias and the limits of agreement are the same for both the Formetta and Li methods. This occurs because, in both cases, they use the same data to calculate R_n (T_{air} and T_c); therefore, the difference in R_n calculated from T_{air} and T_c is expected to be the same. The bias at the hourly and daily scales were -4.82 and -4.91 W m^{-2}, respectively, indicating that estimating R_n using T_{air} results in an average difference of approximately – 5.0 W m^{-2} under well-watered conditions. Thus, for practical purposes-and considering the modest improvement obtained by using T_c instead of T_{air} (Fig. 8) the assumption of similarity may be particularly reasonable at the daily time scale, when the differences between T_c and T_{air} are also expected to be minimal (Fig. 11).

The differences between T_{air} and T_c were largest at the hourly scale (Fig. 11), as expected, with an average difference (T_c – T_{air}) of -0.82°C and a peak difference of -8.7°C, indicating that T_{air} was generally slightly higher than T_c. Nevertheless, at the daily scale, the differences were less pronounced, with a peak difference of -3.4°C, which reinforced the use of T_{air} to estimate emitted longwave radiation at R_n estimation.

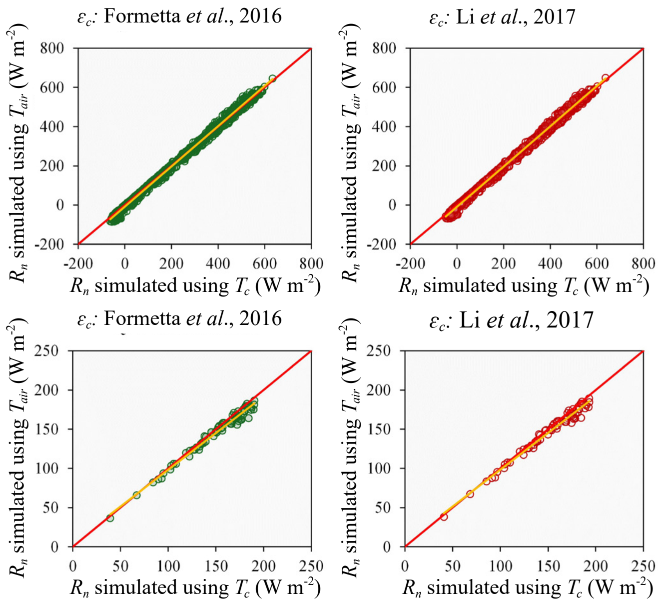

Fig. 9. Linear regression comparing R_n estimates obtained from T_{air} and T_c with different models used to calculate ε_c. The red line indicates the 1:1 line, and the yellow line represents the regression line.

Table 3. Results of linear regression analysis comparing R_n estimates derived from T_{air} and T_c across different time scales and using various methods

Variable	Model	Intercept			Slope		
		Value	Lower 95%	Upper 95%	Value	Lower 95%	Upper 95%
Hourly (T_{air} *vs* T_c)	Formetta	-8.427*	-8.982	-7.873	1.027*	1.025	1.029
	Li	-8.794*	-8.221	-9.366	1.028*	1.025	1.030
Daily (T_{air} *vs* T_c)	Formetta	4.636^{ns}	-0.381	9.653	0.937*	0.904	0.969
	Li	4.566^{ns}	-0.486	9.617	0.938*	0.906	0.970

*Significant at p <0.001, ns – not significant (p > 0.05).

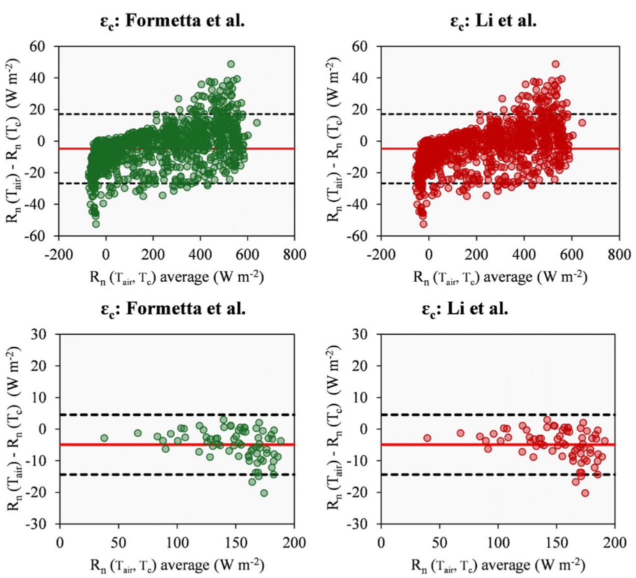

Fig. 10. Bland-Altman plot comparing R_n estimates using T_{air} and T_c, as well as different models for calculating ε_c. The upper and lower dashed lines indicate the limits of agreement, and the red line represents the Bias (Formetta *et al.*, 2016; Li *et al.*, 2017).

Although comparable studies in literature are scarce, similar results were reported by Carrasco and Ortega-Farías (2008), who evaluated two models to estimate R_n in vineyards (*Vitis vinifera* cv. Cabernet Sauvignon), considering either T_{air} as a substitute for T_c or the actual T_c. Their results showed that the model using T_{air} was able to estimate net radiation with a good degree of precision, although the temperature gradient between the canopy and the air ranged from –3 to 4°C, indicating that the incorporation of canopy temperature did not substantially improve R_n estimation, provided that soil water content were maintained at an optimum level to minimize the temperature differences.

This study focused exclusively on the substitution of T_{air} for T_c under well-watered conditions. However, no threshold was identified to define the temperature difference beyond which T_{air} and T_c can no longer be used interchangeably. This aspect requires further investigation, since R_n is also required in energy balance studies under non-irrigated or water-stressed crop conditions. The acceptable temperature difference threshold likely depends on several factors, primarily soil water content. Previous studies have shown

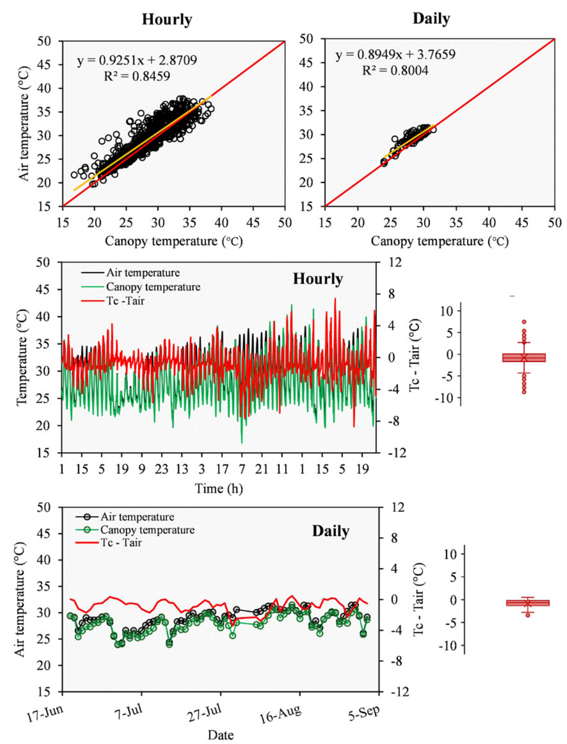

Fig. 11. Relationship between air temperature (T_{air}, °C) and canopy temperature (T_c, °C) at hourly and daily time scales in a cotton field at Uvalde during 2025. The boxplot on the right shows the distribution of errors at each time scale.

that reductions in soil water content can lead to increases in canopy temperatures of up to 10°C higher than air temperature (Luan and Vico, 2021). Therefore, additional research is necessary to determine the critical threshold at which substituting T_{air} for T_c becomes inappropriate.

4. CONCLUSIONS

In this study, we investigated whether net radiation (R_n) estimation could be improved by applying the Brunt approach for clear-sky emissivity, as previously calibrated by Formetta *et al.* (2016) and Li *et al.* (2017). Additionally, we examined whether air temperature (T_{air}) could substitute canopy temperature (T_c) in cotton crops under well-watered conditions. The results show that both clear-sky emissivity models improved R_n estimation compared with the original Allen equation, eliminating the need for site-specific calibration. Regarding the substitution of T_c with T_{air}, we found that the improvement achieved by using T_c was modest, particularly at the daily time scale. Thus, under wellwatered conditions, R_n can be satisfactorily estimated using T_{air} as a substitute for T_c, especially at the daily time scale. The broader scientific significance of this work lies in validating that T_{air} can reliably serve as a proxy for T_c in well-watered crops at the daily scale. This finding offers practical utility for regional-scale agricultural modeling and crop water management.

Conflict of interest. The authors have no conflicts of interest to disclose.

Acknowledgments. We appreciate Ray King, Bethany Speer, Sixto Silva, Dalton Thompson, Angela Jones, Joe Gonzalez and Randy Cox for assistance in crop management and field sample collection, and Christine Thompson and Liza Silva for administrative support. We thank the late Professor Dr. J. Tom Cothren for advice on cotton variety selection for the 2015 cotton trial and appreciate the help from Dale A. Mott for providing seeds for the 2025 cotton trial. We thank Dr. Charles Stichler for advice on sesame management.

CRediT authorship contribution statement. Thiago F. Duarte: writing – original draft, Writing – review and editing, conceptualization, data curation, visualization, software, methodology, investigation, formal analysis, validation, funding acquisition. Xuejun Dong: writing – review and editing, conceptualization, methodology, investigation, data curation, validation, supervision, resources, funding acquisition, project administration. Uzair Ahmad: writing – review and editing, data curation, investigation. Noemi Tortorici: writing – review and editing, data curation, investigation. Tonny J.A. Silva: methodology, validation, writing – review and editing. Edna M. Bonfim-Silva: methodology, validation, writing – review and editing. Daniel I. Leskovar: methodology, funding acquisition, writing – review and editing. All authors have read and agreed to the published version of the manuscript.

Data accessibility. The dataset in support of this work is available at https://zenodo.org/records/19118881

5. REFERENCES

Allen, R.G., Pereira, L.S., Raes, D., Smith, M., 1998. Crop evapotranspiration – Guidelines for computing crop water requirements. FAO Irrigation and Drainage Paper 56. FAO, Rome.

Allen, R.G., Smith, M., Pereira, L.S., Perrier, A., 1994. An update for the calculation of reference evapotranspiration. ICID Bull. 43(2), 35-92.

An, N., Hemmati, S., Cui, Y.J., 2017. Assessment of the methods for determining net radiation at different time-scales of meteorological variables. J. Rock Mech. Geotech. Eng. 9(2), 239-246. https://doi.org/10.1016/j.jrmge.2016.11.001

Bland, J.M., Altman, D.G., 1986. Statistical methods for assessing agreement between two methods of clinical measurement. Lancet 1, 307-310. https://doi.org/10.1016/S0140-6736(86)90837-8

Blonquist Jr., J.M., Allen, R.G., Bugbee, B., 2010. An evaluation of the net radiation sub-model in the ASCE standardized reference evapotranspiration equation: Implications for evapotranspiration prediction. Agric. Water Manag. 97(7), 1026-1038. https://doi.org/10.1016/j.agwat.2010.02.008

Blonquist Jr., J.M., Norman, J.M., Bugbee, B., 2009. Automated measurement of canopy stomatal conductance based on infrared temperature. Agric. For. Meteorol. 149(12), 2183-2197. https://doi.org/10.1016/j.agrformet.2009.06.021

Bristow, K.L., 1987. On solving the surface energy balance equation for surface temperature. Agric. For. Meteorol. 39(1), 49-54. https://doi.org/10.1016/0168-1923(87)90022-0

Brunt, D., 1932. Notes on radiation in the atmosphere I. Q. J. R. Meteorol. Soc. 58, 389-420. https://doi.org/10.1002/qj.49705824704

Brutsaert, W., 1975. On a derivable formula for long-wave radiation from clear skies. Water Resour. Res. 11(5), 742-744. https://doi.org/10.1029/WR011i005p00742

Bsaibes, A., Courault, D., Baret, F., Weiss, M., Olioso, A., Jacob, F., *et al.*, 2009. Albedo and LAI estimates from FORMOSAT-2 data for crop monitoring. Remote Sens. Environ. 113(4), 716-729. https://doi.org/10.1016/j.rse.2008.11.014

Campbell, G.S., Norman, J.M., 1998. Radiation fluxes in natural environments. In: An Introduction to Environmental Biophysics. Springer, New York, 167-184.

Carmona, F., Rivas, R., Caselles, V., 2014. Estimation of daytime downward longwave radiation under clear and cloudy skies conditions over a sub-humid region. Theoret. Appl. Climatol. 115(1-2), 281-295.

Carvalho, H.D.R., McInnes, K.J., Heilman, J.L., *et al.* Radiative balance and temperature of differently pigmented cotton canopies. Int. J. Biometeorol. 66, 591-600 (2022). https://doi.org/10.1007/s00484-021-02221-x

Carrasco, M., Ortega-Farías, S., 2008. Evaluation of a model to simulate net radiation over a vineyard cv. Cabernet Sauvignon. Chil. J. Agric. Res. 68, 156-165. https://doi.org/10.4067/S0718-58392008000200007

Crawford, T.M., Duchon, C.E., 1999. An improved parameterization for estimating effective atmospheric emissivity for use in calculating daytime downwelling longwave radiation. J. Appl. Meteorol. 38(4), 474-480. https://doi.org/10.1175/1520-0450(1999)038<0474:AIPFEE>2.0.CO;2

Flerchinger, G.N., Xiao, W., Marks, D., Sauer, T.J., Yu, Q., 2009. Comparison of algorithms for incoming atmospheric long-wave radiation. Water Resour. Res. 45(3), W03423. https://doi.org/10.1029/2008WR007394

Formetta, G., Bancheri, M., David, O., Rigon, R., 2016. Performance of site-specific parameterizations of longwave radiation. Hydrol. Earth Syst. Sci. 20(11), 4641-4654. https://doi.org/10.5194/hess-20-4641-2016

Gupta, H.V., Kling, H., Yilmaz, K.K., Martinez, G.F., 2009. Decomposition of the mean squared error and NSE performance criteria: Implications for improving hydrological modelling. J. Hydrol. 377(1-2), 80-91. https://doi.org/10.1016/j.jhydrol.2009.08.003

He, T., Gao, F., Liang, S., Peng, Y., 2019. Mapping climatological bare soil albedos over the contiguous United States using MODIS data. Remote Sens. 11(6), 666. https://doi.org/10.3390/rs11060666

Holmes, T.R.H., Owe, M., De Jeu, R.A.M., Kooi, H., 2008. Estimating the soil temperature profile from a single depth observation: A simple empirical heatflow solution. Water Resour. Res. 44(2), W02407. https://doi.org/10.1029/2007WR005994

Idso, S.B., Jackson, R.D., 1969. Thermal radiation from the atmosphere. J. Geophys. Res. 74(23), 5397-5403. https://doi.org/10.1029/JC074i023p05397

Jackson, R.D., Idso, S.B., Reginato, R.J., Pinter Jr., P.J., 1981. Canopy temperature as a crop water stress indicator. Water Resour. Res. 17(4), 1133-1138. https://doi.org/10.1029/WR017i004p01133

Jensen, M.E., Allen, R.G., 2016. Evaporation, evapotranspiration, and irrigation water requirements. ASCE Manuals and Reports on Engineering Practice No. 70. ASCE, Reston, VA.

Jensen, M.E., Burman, R.D., Allen, R.G. (Eds), 1990. Evapotranspiration and Irrigation Water Requirements. ASCE Manuals and Reports on Engineering Practice No. 70. ASCE, New York.

Kjaersgaard, J.H., Cuenca, R.H., Plauborg, F.L., Hansen, S., 2007. Long-term comparisons of net radiation calculation schemes. Boundary-Layer Meteorol. 123(3), 417-431. https://doi.org/10.1007/s10546-006-9149-2

Li, M., Jiang, Y., Coimbra, C.F.M., 2017. On the determination of atmospheric longwave irradiance under all-sky conditions. Sol. Energy 144, 40-48. https://doi.org/10.1016/j.solener.2017.01.002

Linacre, E.T., 1969. Net radiation to various surfaces. J. Appl. Ecol. 6, 61-75. https://doi.org/10.2307/2401297

Lipiec, J., Usowicz, B., 2021. Quantifying cereal productivity on sandy soil in response to some soil-improving cropping systems. Land 10(11), 1199. https://doi.org/10.3390/land10111199

Luan, X., Vico, G., 2021. Canopy temperature and heat stress are increased by compound high air temperature and water stress and reduced by irrigation – a modeling analysis, Hydrol. Earth Syst. Sci. 25, 1411-1423, https://doi.org/10.5194/hess-25-1411-2021

Monson, R.K., Baldocchi, D.D., 2014. Terrestrial Biosphere-Atmosphere Fluxes. Cambridge University Press.

Morales-Salinas, L., Ortega-Farias, S., Riveros-Burgos, C. *et al.,* 2023. Assessment of atmospheric emissivity models for clear-sky conditions with reanalysis data. Sci. Rep. 13, 14465.

Moriasi, D.N., Arnold, J.G., Van Liew, M.W., Bingner, R.L., Harmel, R.D., Veith, T.L., 2007. Model evaluation guidelines for systematic quantification of accuracy in watershed simulations. Trans. ASABE 50 (3), 885-900.

Myeni, L., Moeletsi, M.E., Clulow, A.D., 2020. Assessment of three models for estimating daily net radiation in southern Africa. Agric. Water Manag. 229, 105951. https://doi.org/10.1016/j.agwat.2019.105951

Pieri, P., 2010. Modelling radiative balance in a row-crop canopy: Row-soil surface net radiation partition. Ecol. Model. 221(5), 791-801. https://doi.org/10.1016/j.ecolmodel.2009.11.012

Snyder, R.L., Eching, S., 2002. Penman-Monteith (hourly) reference evapotranspiration equations for estimating ETos and ETrs with hourly weather data. Regents of the University of California, Davis.

Usowicz, B., Lipiec, J., Łukowski, M., Bis, Z., Usowicz, J., Latawiec, A.E., 2020. Impact of biochar addition on soil thermal properties: Modelling approach. Geoderma 376, 114574. https://doi.org/10.1016/j.geoderma.2020.114574

Yellareddygari, S.K.R., Gudmestad, N.C., 2017. Bland-Altman comparison of two methods for assessing severity of Verticillium wilt of potato. Crop Prot. 101, 68-75. https://doi.org/10.1016/j.cropro.2017.07.008